Journal of Food Engineering 91 (2009) 319–324

Contents lists available at ScienceDirect

Journal of Food Engineering

journal homepage: www.elsevier.com/locate/jfoodeng

Ripeness and rot evaluation of 'Tommy Atkins' mango fruit through volatiles detection

Zhenfeng Li [a,*], Ning Wang [b], G.S. Vijaya Raghavan [a], Clément Vigneault [c]

[a] Department of Bioresource Engineering, McGill University, 21111 Lakeshore Road, Ste-Anne-de-Bellevue, QC, Canada H9X 3V9
[b] Biosystems and Agricultural Engineering, Division of Agricultural Sciences and Natural Resources, Oklahoma State University, 111 Ag Hall, Stillwater, OK 74078, USA
[c] Horticulture Research and Development Center, Agriculture and Agri-food Canada, 430 Gouin Blvd., Saint-Jean-sur-Richelieu, QC, Canada J3B 3E6

ARTICLE INFO

Article history:
Received 1 June 2008
Received in revised form 9 September 2008
Accepted 12 September 2008
Available online 21 September 2008

Keywords:
zNose™
Mango
Volatiles
Rot
Ripeness
PLS
VIP

ABSTRACT

An ultra fast GC (zNose™), based on an uncoated surface acoustic wave sensor, was employed to detect the volatiles of 'Tommy Atkins' mango fruits. The detected volatile signals were used to identify rot occurrence and evaluate mango ripeness during shelf life. Respiration rate, color, and total soluble solids (TSS) were measured accordingly to indicate mango quality status. Two peaks detected with the zNose™ predicted rot occurrence with 90% and 87% accuracy, respectively, while another peak was 80% accurate in predicting ripeness with respect to a reference color index. Partial least squares (PLS) regression combined with variable importance for projection (VIP) was used to select the peaks important in prediction. The rot prediction methods could have potential applications in the mango industry for the diagnosis of the occurrence of mango rots.

1. Introduction

Mango [*Mangifera indica* L.] is one of the most important tropical fruits marketed throughout the world. The fruits are normally harvested at the green mature stage and then transported and stored at low temperatures (10–15 °C) to extend their shelf life (Snowdon, 1990). However, severe post-harvest diseases still occur, resulting in rot contributing to substantial post-harvest losses (Beyers et al., 1979; Pantastico et al., 1984; Pesis et al., 2000). Hence, there is a need to monitor the disease severity and rot occurrence during the shelf life of mangoes in order to prevent the spread of diseases. Evaluating maturity and ripeness is another important issue for mango industry. Presently the pre-harvest maturing of mango fruits is estimated by size, sphericity, firmness, total soluble solids (Jha et al., 2006) and post-harvest ripening is often evaluated by respiration rate, skin color (Lalel et al., 2003), texture softening (Yashoda et al., 2006), etc.

An attractive flavor is one of the characteristics that make mango a highly prized fruit. The varying flavor at different stages of harvest and after certain storage time is not only distinguishable by human senses, but also reflects physiological and biochemical changes. Some studies of different mango cultivars' volatiles have been undertaken (Macleod and de Troconis, 1982; Macleod and Pieris, 1984; Idstein and Schreier, 1985), and flavors at different developmental stages have also been compared (Ibanez et al., 1998; Lalel et al., 2003). Unfortunately, all the methods used in these studies, including GC, GC/MS and SPME, are labour and time intensive, making their application outside the laboratory almost impossible.

In recent years, electronic noses have been employed to evaluate fruit flavor, and a number of applications for different fruits have been reported: apple (Saevels et al., 2004), mandarin (Gomez et al., 2006), orange (Natale et al., 2001), and peach (Natale et al., 2002). In terms of mango, Lebrun et al. (2008) recently achieved partial success in using an e-nose FOX 4000 to discriminate mango maturity. However, no fast and practical method has been reported for ripeness and rot prediction.

In this study, an ultra fast portable GC (zNose™) was employed to detect mango volatiles. The specific objectives were:

(1) To predict rot occurrence of mango fruits by detecting volatile signals;
(2) To evaluate mango ripeness over the period of their shelf life.

* Corresponding author. Tel.: +1 514 398 4400/7632; fax: +1 514 398 8387.
E-mail address: zhenfeng.li@mail.mcgill.ca (Z. Li).

0260-8774/$ - see front matter © 2008 Elsevier Ltd. All rights reserved.
doi:10.1016/j.jfoodeng.2008.09.009

Nomenclature

B	predictor coefficient in PLS regression model
Cts	counts
GC	gas chromatography
GC/MS	gas chromatography/mass spectrometry
PLS	partial least square
RR	respiration rate
RT	retention time
SAW	surface acoustic wave
SPME	solid phase microextraction
TSS	total soluble solids
VIP	variable importance for projection

2. Materials and methods

2.1. Experimental materials and procedure

One hundred and twenty mango fruits of cv. 'Tommy Atkins' (*Cocanmex S.A. de C.V.*), selected to be as green as possible, were obtained from a local fruit distribution company (Aliments IMAX Foods Inc., Montreal, Quebec) and stored at room temperature (20–22 °C) without any treatment. Twelve mangoes were used as control samples and the remaining 108 as regular samples. The control samples were measured every day for 31 days until all were rotten. In contrast, the 108 regular samples were randomly chosen, measured, and then discarded.

Airtight glass jars (2.3 l) were used for both respiration rate (RR) and volatile measurements. An aperture was made in the metal cover, fitted with a rubber septum for gas sampling and sealed with Teflon sealant. The containers were tested to be free of zNose™-detectable volatiles when empty. A single mango was put in a container for 2 h at room temperature (20–22 °C), prior to measurement. This equilibrium time was obtained from preliminary experiments where, in 10 h, the volatiles signal reached 80% of its highest value within 2 h (results not shown). Fruit weight was measured with an electronic scale.

2.2. Respiration rate (RR)

Gas samples (5 mL each) were taken from the glass jar, CO_2 and O_2 were measured with a SRI 8610A Gas Chromatograph (SRI Instruments Inc., Las Vegas, USA). The sensor temperature of the Gas Chromatograph was set to 55 °C and the flow pressure was 70 psi (482 kPa). The measured RR was compared with the volatile profiles acquired from the zNose™ in an attempt to assess ripeness of mango fruits. All measurements were repeated twice and mean values are reported.

2.3. Volatile detection system

A zNose™ (7100 Fast GC Analyzer, Electronic Sensor Technology, New Bury Park, CA, USA) was used for volatile compound detection. It is actually a miniature, high-speed gas chromatograph (GC) containing a detector, a short separation column, and support electronics.

The detector of the zNose™ is an uncoated, high quality surface acoustic wave (SAW) crystal. The crystal operates by maintaining high frequency acoustic waves on its surface. The targeted compound lands and sticks on the detector and changes its frequency. The frequency change is measured by a microcontroller and processed by software, allowing the compound to be identified and quantified.

Before the volatile compounds reach the detector, they are separated by a short column (DB-5). The time a given component remains in the column is recorded as its retention time (RT), which is supposed to be unique for each specific chemical, while the derivative of frequency signal is used as a quantitative measurement of the quantity of the chemical (area under a peak, expressed in Counts).

The zNose™ employs headspace and bubbler techniques as its sampling modes. A side Luer needle was used as a sample odour injection tool, and a spark needle as the bubbler generator. A rotating valve was used to switch the machine from sampling configuration to an inject configuration. A trap was used as a preconcentrator to collect and hold volatile samples, and high grade helium was used as the sample carrier gas.

All samples in this experiment were tested using the following mode of operation: sampling through side Luer needle for 10 s, separating different compounds in the column for 14 s, acquiring a frequency signal every 0.02 s for 20 s, and baking the sensor for 30 s. The sensor detection temperature was set to 60 °C. Column temperature was ramped from 40 °C to 180 °C at the rate of 10 °C s^{-1}, while the sensor baking temperature was 150 °C. The carrier gas flowed at a rate of 3.0 cm^3 s^{-1}. Between each measurement, at least one air blank was run, such that baseline peaks were all under 200 Counts before resuming sample runs. All measurements were repeated twice and mean values are reported.

2.4. Subjective assessments of ripeness and rot

Disease severity was assessed by evaluating the percentage of fruit surface covered by black lesions (Kobiler et al., 2001). The arc length of a lesion was measured with a soft ruler and the surface area of the spherical calotte was calculated, and thus the corresponding percentage obtained. However, as the lesions did not present a perfectly spherical calotte and the mango fruits were not perfect spheres, the calculated percentage value was assigned to the nearest 5% step percent (i.e., 0%, 5%, 10%, etc.) by combining visual observations. The degree of rot was continuously monitored until 50–70% of the surface area was damaged.

Ripeness development was assessed by viewing the mango fruit's skin. A color index was recorded according to the following rating scale (Shorter and Joyce, 1998): (1) 100% green; (2) 75% green; (3) 50% green and 50% yellow; (4) 75% yellow; (5) 100% yellow. The color index was proportionally converted from a percentage to a numerical value to facilitate comparison with respiration rate and volatile signals.

2.5. Objective color and total soluble solids (TSS) measurements

The skin color of mango samples was also measured with a tristimulus colorimeter (Chroma Meter CR-300, Minolta Co. Ltd., Japan) in the L^*, a^*, b^* color space. Four evenly distributed places along the equator were selected and a mean value was used. Three values were obtained: "L" measures lightness and varies from 100 for perfectly reflective white to zero for perfectly absorptive black; "a" measures redness when positive, gray when zero, and greenness when negative; and "b" measures yellowness when positive, gray when zero, and blueness when negative.

Total soluble solids (TSS) of 108 regular samples were measured with a handheld refractometer (ERMA, Japan) after RR, volatiles, and color measurements. Four pieces of flesh were drawn from

1 cm below the locations of colorimeter measurements and juice hand-squeezed from them for TSS measurements. Mean TSS values were used for computation of a maturity index (I_m,%) as follows: $I_m = (TSS/8) \times 100$ (Jha et al., 2007). A correlation analysis of colorimeter readings and I_m was attempted.

2.6. Statistical analysis

Data analysis was carried out using SAS version 9.1 (SAS Institute Inc., Cary, NC, USA). Partial least squares (PLS) regression combined with variable importance for projection (VIP) was adopted to select the most important peaks for rot prediction and ripeness evaluation. The predictor coefficient (B) in PLS regression model represents the contribution of a predictor to the response only, while VIP represents the importance of each predictor in fitting the PLS model for both predictors and response (Chong and Jun, 2005; Wold, 1994). If a predictor has a relatively greater coefficient (in absolute value) and a greater value of VIP, it is selected as an important predictor.

3. Results and discussion

3.1. Preliminary volatiles estimation

Total ten obvious peaks were detected by zNose™ from unripe, ripe, and overripe mango samples. The volatile profiles of a representative sample (control sample 8) at 24 days are depicted in Fig. 1. All other samples had similar profiles with quantitative differences. As Peaks a–c only appeared when the mango fruits were fully rotten and beyond the scope of this study, only Peaks 1–7 will be discussed.

By close observations of the 7 peaks, it can be found that Peaks 1, 3, 4, and 5 increased with storage time, $Peak_2$ first decreased then increased, $Peak_6$ decreased all the way, $Peak_7$ increased first and then decreased. These variations in volatile compounds may relate to the biochemical changes in mango fruits and may represent different stages of mango ripeness and rot development. After comparing with RR and subjective assessments, Peaks 4, 5, and 7 were tentatively chosen as key parameters for ripeness evaluation and rot prediction. Fig. 2 shows the development of Peaks 4, 5, and 7 in control sample 8 at 24 days. The corresponding RR, observed rots percentage, and subjective color assessments are also shown in Fig. 2. To facilitate comparison with RR and observed rots percentage values, original volatile signals, i.e., peak areas were modified as: peak areas × 0.005.

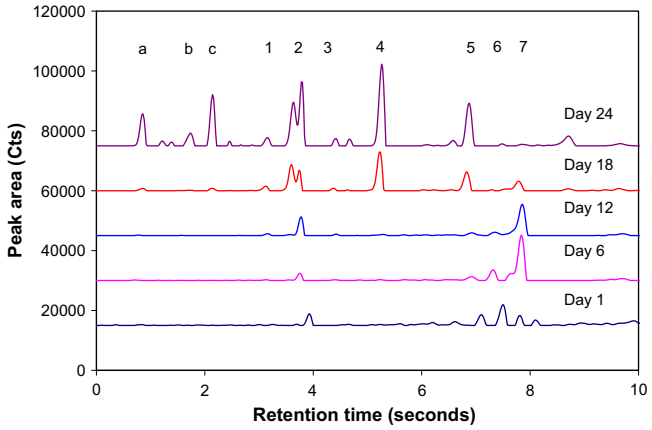

Fig. 1. Volatile profiles of control sample 8 (Different retention times represent different components and the corresponding peak's area represents the quantity; the baselines of these profiles were increased according to date sequence).

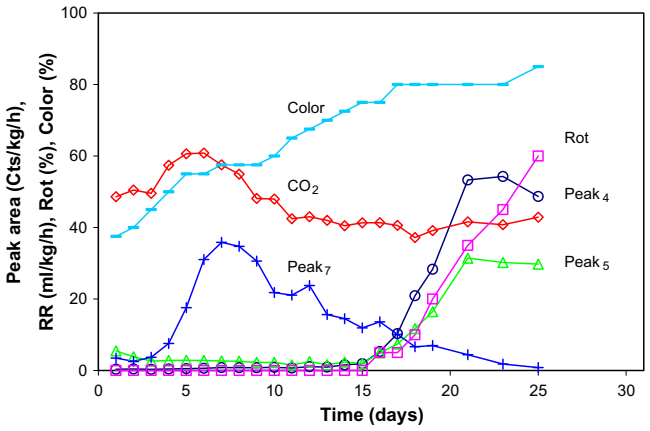

Fig. 2. Peaks 4, 5, 7 and RR, rot, color assessments of control sample 8 (Measurements were duplicated and mean values are reported; peak values were timed with a coefficient of 0.005).

By close observation of Fig. 2, one sees that Peaks 4 and 5 increased almost at the same time as did the degree of rot, while $Peak_7$ was tightly related to RR and subjective color assessment. These trends imply that $Peak_4$ and $Peak_5$ may be related to mangoes' rotting status, while $Peak_7$ may be related to mangoes' ripeness development.

3.2. Rot prediction

The potential of predicting rot occurrence with $Peak_4$ and $Peak_5$ was tried first. The curves of $Peak_4$, $Peak_5$, and observed rotting of the 12 control samples are presented in Fig. 3. For samples 1, 5, 6, 7, and 10, $Peak_4$ and $Peak_5$ increased along with the increase in observed rot, while for samples 2, 3, 8, 9, 11, 12, the appearance of $Peak_4$ and $Peak_5$ preceded observed rot. Only the volatile signals of sample 4 appeared 1 day later than observed rots. Hence, the occurrence of rot in mango fruits can possibly be predicted with $Peak_4$ and $Peak_5$.

To statistically testify the importance of $peak_4$ and $peak_5$ for rot prediction, PLS regression combined with VIP was conducted for 108 regular samples. Area values of $peak_1$–$peak_7$ were used as predictors and the observed rot percentage as response. $Peak_4$ and $peak_5$ showed the greatest B and VIP values (Table 1); hence they were selected as the most important predictors for rot occurrence.

To devise a practical way to categorically assess a mango as rotten, the threshold values of $peak_4$ and $peak_5$ were acquired as follows: among all the 120 samples, when a mango first present rotten symptom and its lesions cover $\leqslant$5% surface area of the fruit, its $peak_4$ and $peak_5$ values were selected and the means of them were obtained (4.76 for $peak_4$ and 4.14 for $peak_5$; from 16 qualified samples). If a mango's $Peak_4$ value exceeded 4.76 and its rot was visually apparent, the sample was considered correctly classified as a rotten mango. On the other hand, if a sample mango's $Peak_4$ value was <4.76 and there was no lesion on the surface, it was correctly classified as non-rotten mango. Otherwise the classification was considered incorrect.

When 108 regular samples were classified as to the presence or absence of lesions, using $Peak_4$ levels, 9 rotten mangoes in 95 samples were misclassified as non-rotten and 2 non-rotten mangoes in 13 samples were misclassified as rotten, equalling a percent correct of 90%. A similar attempt of rot prediction in 108 regular samples using $Peak_5$ showed a misclassification of non-rotten mangoes in 11 of 96 cases, and the misclassification of rotten mangoes in 3 of 12 samples. In total, 14 in 108 samples were misclassified corresponding to 87% accuracy.

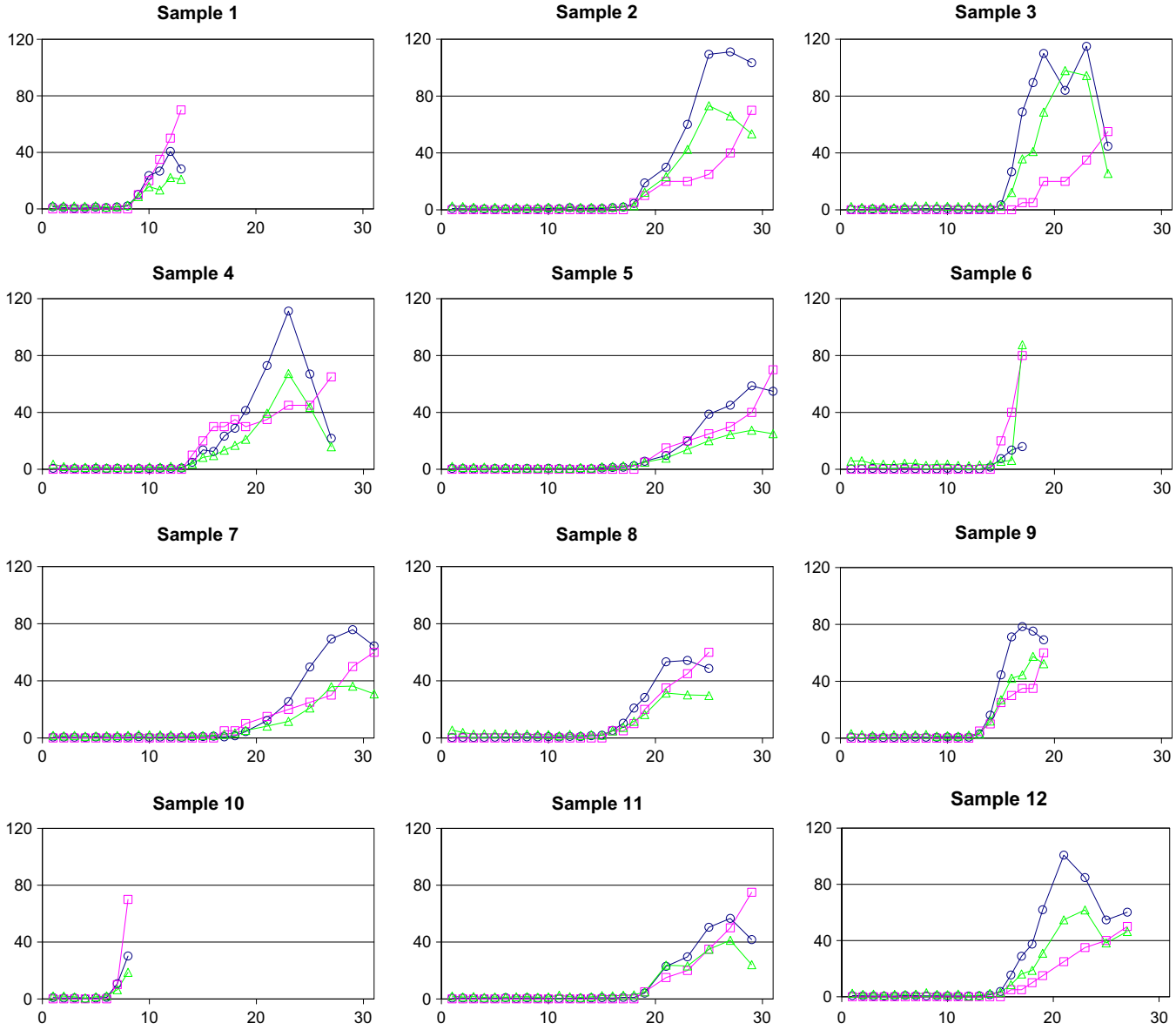

Fig. 3. Rot prediction with $Peak_4$ and $Peak_5$ in 12 control samples [□, Observed rots (%); ○, $Peal_4$ (Cts/kg/h); Δ, $Peak_5$ (Cts/kg/h)] [X axis: time (days)] (Measurements were duplicated and mean values were reported; peak values were timed with a coefficient of 0.005).

Table 1
PLS analysis for rot prediction

Predictors	B[a]	VIP[b]
$Peak_1$	0.08388	0.93411
$Peak_2$	−0.00022	0.89754
$Peak_3$	0.05316	1.18948
$Peak_4$	0.25066	2.16771
$Peak_5$	0.26851	2.23243
$Peak_6$	−0.24154	1.48823
$Peak_7$	0.01338	0.09716

[a] Predictor coefficient in PLS regression model.
[b] Variable importance for projection.

Similar results were reported by Moalemiyan et al. (2007) for mango cv. Keitt. Using GC/MS to analyze volatile organic compounds, they found 1-Patenol to be symptomatic of stem end rot and thujol of anthracnose infection. Although volatile compounds are cultivar dependent, similar observations in these two studies confirmed that the prediction of mango rot by way of volatile organic compounds is a promising method for mango industry. However, their observations were not consistent for all replicates, whereas in this study a high accuracy of rot prediction was achieved. Moreover, GC/MS usually requires hours of operation for volatiles measurements, whereas the volatiles measurement with zNose™ only requires a few minutes.

3.3. Ripeness evaluation

The possibility of predicting mango ripeness with $Peak_7$ was also evaluated, with the 12 control samples as a first attempt. To avoid disturbance by rot signals, only measurements from fruit without rot symptoms were used, i.e., any fruit-measurement where rot was observed, or $Peak_4$ exceeded 4.76, or $Peak_5$ exceeded 4.14 was removed, leaving a total of 167 fruit-measurements. The respiration rate, subjective color assessments, and $Peak_7$ values of the 12 control samples' 167 measurements are presented in Fig. 4.

Increases in RR of control samples were all followed by increases in $Peak_7$, sometimes soon, sometimes later. As the

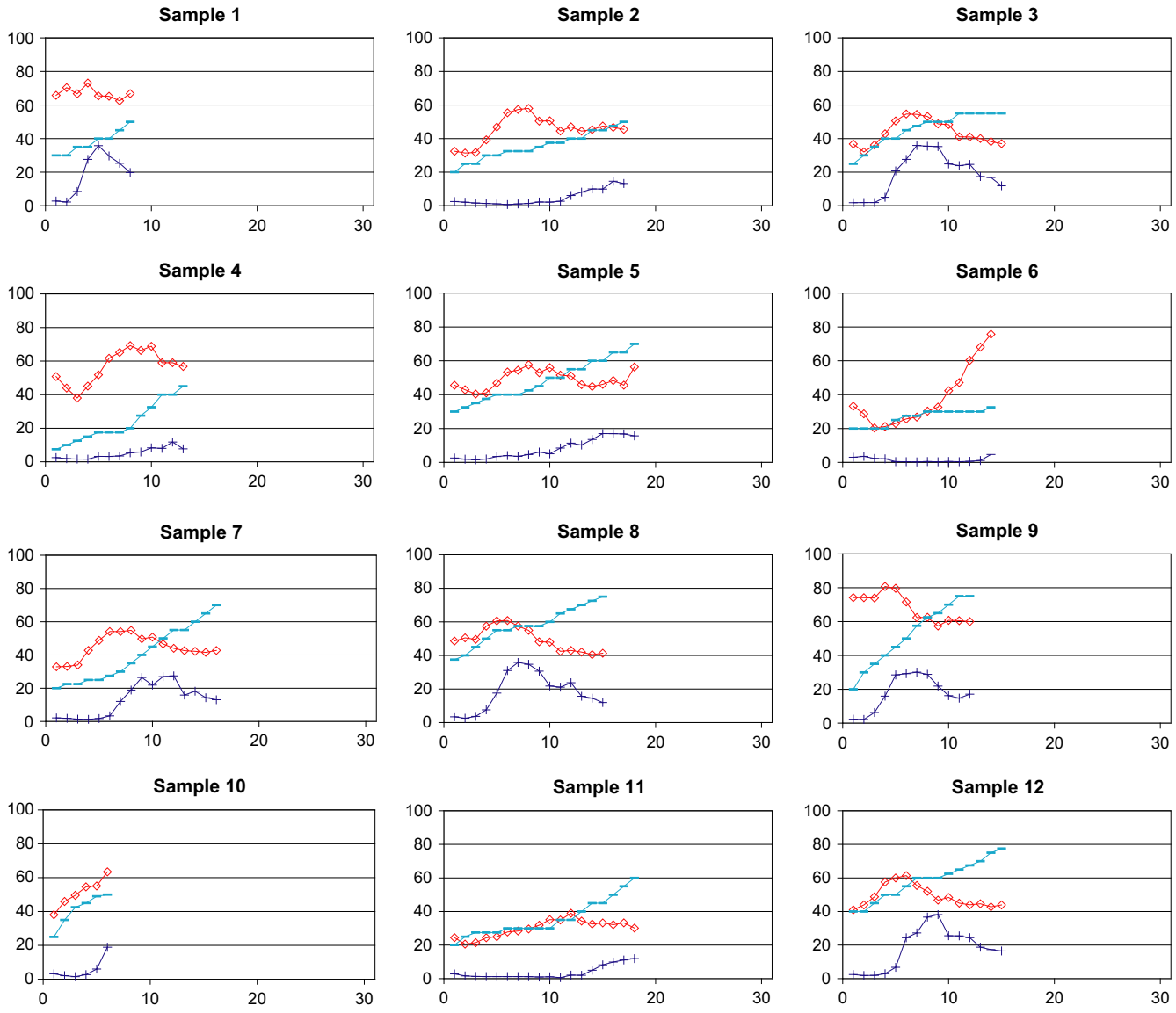

Fig. 4. Ripeness evaluation of 12 control samples using $Peak_7$ [−: observed colour (%); ◇: RR (ml/kg/h); +: $Peak_7$ (Cts/kg/h)] [X axis: time (days)] (Measurements were duplicated and mean values were reported; peak values were timed with a coefficient of 0.005).

climacteric rise is a characteristic phenomenon of the ripening process (Biale et al., 1954), RR and $Peak_7$ might be used as parameters for ripeness evaluation. However, RR values varied widely among different samples, although for a single mango the RR has a climacteric peak. For example, RR of sample 1 was between 60 and 80 ml kg^{-1} h^{-1}, but the RR of sample 11 was between 20 and 40 ml kg^{-1} h^{-1}. The lowest value of sample 1 was larger than the highest value of sample 11. Hence, RR can not be used as a general rule to judge mango ripeness. By contrast, the $Peak_7$ value increased from near zero to higher values and has the potential to be used for estimation of mango ripeness. To estimate the potential of evaluating mango ripeness with $Peak_7$, the subjective color assessment was employed as the ripeness reference (Biale et al., 1954). A sample was considered ripe when 50 ± 5% of its skin was yellow. The TSS was not adopted for reasons which will be outlined below.

Among 108 regular samples, there were 82 rot-free samples according to the previous criteria. To statistically confirm the importance of $peak_7$ in ripeness evaluation, PLS regression combined with VIP was conducted (Table 2). Clearly $peak_7$ had both the greatest B and VIP values; hence it is the most important variable for ripeness evaluation.

Table 2
PLS analysis for ripeness prediction

Predictors	B[a]	VIP[b]
$Peak_1$	0.00699	0.43578
$Peak_2$	−0.01528	1.08673
$Peak_3$	−0.03755	1.09540
$Peak_4$	0.02644	0.33066
$Peak_5$	0.06809	0.49863
$Peak_6$	−0.04881	0.34008
$Peak_7$	0.42289	3.45768

[a] Predictor coefficient in PLS regression model.
[b] Variable importance for projection.

Similar to rot prediction, a threshold of $peak_7$ was selected as follows: when a rot-free mango's color index reached 50 ± 5%, it was considered to be starting the ripening process, and the mean $peak_7$ value was taken as the threshold (from 19 qualified samples). An analysis of the 82 rot-free samples for ripeness

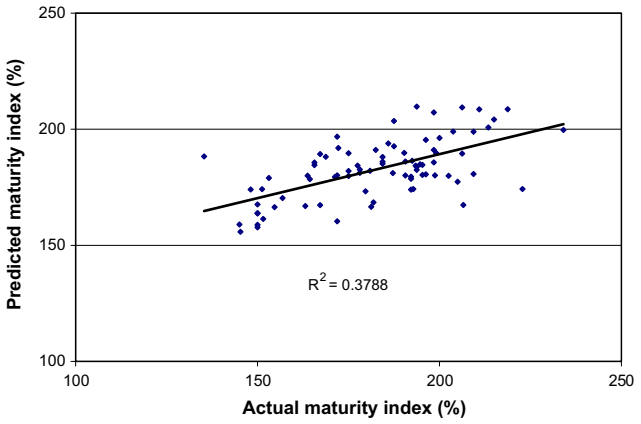

Fig. 5. Relationship between TSS-predicted and actual maturity index.

evaluation using $Peak_7$ showed 10 of 46 unripe mangoes were misclassified, as were 6 of 36 ripe mangoes, resulting in an overall accuracy of 80%.

Lalel et al. (2003) reported similar observations for 'Kensington Pride' mangoes. Respiration rate (CO_2 production) reached a peak of 50.75 ml kg^{-1} h^{-1} on the fourth day of ripening and a ripe skin color occupied 75% of the total fruit surface area by the seventh day, thereafter color change slowed down. With SPME–GC–FID and SPME–GC–MS techniques, they found that the major monoterpenes (*α-Terpinolene*) increased in the first 3 or 4 days and decreased thereafter when the fruit became overripe. This behavior is very similar to that observed for $Peak_7$ in the current study.

3.4. TSS and objective color

The relationship between TSS and objective color was investigated for the 82 regular rot-free samples (Fig. 5). The "a", "b", and "a^* b" values were used in a multiple linear regression model (Jha et al., 2007) to predict TSS index. Unfortunately, an $R^2 = 0.38$ ($P < 0.0001$) resulted, indicating that TSS cannot be predicted with objective color. The reason might be that a full development of TSS occurred during 1–2 week transportation from Mexico to Canada, since measured TSS of all 108 regular samples exceeded 8 Brix°. Hence, TSS is not a good index for ripeness evaluation during shelf life, although it could be used to predict mango maturity during harvesting period. This inversely proved that the evaluation of mango volatiles is the only viable method for ripeness estimation.

4. Conclusions

Volatile signals detected with zNose™ are useful parameters for mango quality evaluation. Seven marked peaks were identified and three were used in rot prediction and ripeness evaluation. Results showed $Peak_4$ was the best candidate for rot prediction with 90% rots prediction accuracy. $Peak_5$ also achieved a rot prediction accuracy of 87%. Evaluation of ripeness was attempted using $Peak_7$. Using subjective color observations as a reference, 80% ripeness evaluation accuracy was achieved. However, the correlation between measured TSS and its predicted counterpart based on colorimetric measurements was poor and cannot be used for ripeness evaluation during shelf life.

The rot prediction methods developed have the potential to be applied in the mango industry for detecting side and stem end rots during mango shelf life in an ultra rapid manner, after validation under commercial conditions.

Acknowledgements

The authors are grateful to the NSERC (Natural Sciences and Engineering Research Council of Canada) for financial support.

References

Beyers, M., Thomas, A.C., Tonder, A.J.V., 1979. γ-Irradiation of subtropical fruits. 1. Composition Tables of mango, papaya, strawberry, and litchi fruits at the edible-ripe stage. Journal Agriculture and Food Chemistry 27, 37–42.

Biale, J.B., Young, R.E., Olmstead, A.J., 1954. Fruit respiration and ethylene production. Plant Physiology 29 (54), 168–174.

Chong, I., Jun, C., 2005. Performance of some variable selection methods when multicollinearity is present. Chemometrics and Intelligent Systems 78, 103–112.

Gomez, A.H., Wang, J., Hu, G., Pereira, A.G., 2006. Electronic nose technique potential monitoring mandarin maturity. Sensors and Actuators B 113, 347–353.

Ibanez, E., Lopez-Sebastian, S., Ramos, E., Tabera, J., Reglero, G., 1998. Analysis of volatile fruit components by headspace solid-phase microextraction. Food Chemistry 63 (2), 281–286.

Idstein, H., Schreier, P., 1985. Volatile constituents of Alphonso mango (*Mangifera Indica*). Phytochemistry 24 (10), 2313–2316.

Jha, S.N., Kingsly, A.R.P., Chopra, S., 2006. Physical and mechanical properties of mango during growth and storage for determination of maturity. Journal of Food Engineering 72, 73–76.

Jha, S.N., Chopra, S., Kingsly, A.R.P., 2007. Modeling of color values for nondestructive evaluation of maturity of mango. Journal of Food Engineering 78, 22–26.

Kobiler, I., Shalom, Y., Roth, I., Akerman, M., Vinokur, Y., Fuchs, Y., Prusky, D., 2001. Effect of 2, 4-dichlorophenoxyacetic acid on the incidence of side and stem end rots in mango fruits. Postharvest Biology and Technology 23, 23–32.

Lalel, H.J.D., Singh, Z., Tan, S.C., 2003. Aroma volatiles production during fruit ripening of 'Kensington Pride' mango. Postharvest Biology and Technology 27, 323–336.

Lebrun, M., Plotto, A., Goodner, K., Ducamp, M., Baldwin, E., 2008. Discrimination of mango fruit maturity by volatiles using the electronic nose and gas chromatography. Postharvest Biology and Technology 48, 122–131.

Macleod, A.J., de Troconis, N.G., 1982. Volatile flavour components of mango fruit. Phytochemistry 21 (10), 2523–2526.

Macleod, A.J., Pieris, N.M., 1984. Comparison of the volatile components of some mango cultivars. Phytochemistry 23 (2), 361–366.

Moalemiyan, M., Vikram, A., Kushalapp, A.C., 2007. Detection and discrimination of two fungal diseases of mango (cv. Keitt) fruits based on volatile metabolite profiles using GC/MS. Postharvest Biology and Technology 45, 117–125.

Natale, C.D., Macagnano, A., Martinelli, E., Paolesse, R., Proietti, E., D'Amico, A., 2001. The evaluation of quality of post-harvest oranges and apples by means of an electronic nose. Sensors and Actuators B 78, 26–31.

Natale, C.D., Zude-Sasse, M., Macagnano, A., Paolesse, R., Herold, B., D'Amico, A., 2002. Outer product analysis of electronic nose and visible spectra: application to the measurement of peach fruit characteristics. Analytica Chimica Acta 459, 107–117.

Pantastico, E.B., Lam, P.F., Ketsa, S., Yuniarti, Kosittrakul, M., 1984. Post harvest physiology and storage of mango. In: Mendoza, D.B., Wills, R.B.H. (Eds.), Mango: Fruit Development, Postharvest Physiology and Marketing in ASEAN. ASEAN Food Handling Bureau, Kuala Lumpur, pp. 39–52.

Pesis, E., Aharoni, D., Aharon, Z., Ben-Arie, R., Aharoni, N., Fuchs, Y., 2000. Modified atmosphere and modified humidity packaging alleviates chilling injury symptoms in mango fruit. Postharvest Biology and Technology 19, 93–101.

Saevels, S., Lammertyn, J., Berna, A.Z., Veraverbeke, E.A., Natale, C.D., Nicolai, B.M., 2004. An electronic nose and a mass spectrometry-based electronic nose for assessing apple quality during shelf life. Postharvest Biology and Technology 31, 9–19.

Shorter, A.J., Joyce, D.C., 1998. Effect of partial pressure infiltration of calcium into 'Kensington' mango fruit. Australian Journal of Experimental Agriculture 38, 287–294.

Snowdon, A.L., 1990. A Colour Atlas of Post Harvest Diseases and Disorders of Fruits and Vegetables. Fruits, vol 2. Wolfe Scientific Ltd, (p. 302).

Wold, S., 1994. PLS for multivariate linear modeling. In: van de Waterbeemd, H. (Ed.), QSAR: Chemometric Methods in Molecular Design. Methods and Principles in Medicinal Chemistry. Verlag–Chemie, Weinheim, Germany.

Yashoda, H.M., Prabha, T.N., Tharanathan, R.N., 2006. Mango ripening: changes in cell wall constituents in relation to textural softening. Journal of Science and Food Agriculture 86, 713–721.